Fast Analysis of Broadband Electromagnetic Scattering Characteristics of Electrically Large Targets using Precorrected Fast Fourier Transform Algorithm based on Near Field Matrix Interpolation Method

Wei Bin Kong [1,2], Xiao Fang Yang [1], Feng Zhou [1], Jia Ye Xie [3], Chuan Jie Chen [1], Na Li [1], and Wen Wen Yang [4]

[1] College of Information Engineering
Yancheng Optical Fiber Sensing and Application Engineering Technology Research Center
Yancheng Institute of Technology, Jiangsu Yancheng, 224051, China
kongweibin2007@sina.com,

[2] State Key Laboratory of Millimeter Waves
Southeast University, Jiangsu Nanjing, 210096, China

[3] Industrial Center
Nanjing Institute of Technology, Jiangsu Nanjing, 211167, China

[4] School of Information Science and Technology, Nantong University, Jiangsu Nantong, 226019, China

Abstract ─ In this paper, a new method is proposed to analyze the broadband electromagnetic characteristics of electrically large targets by combining the precorrected-FFT algorithm (P-FFT) with the near-field matrix interpolation technique. The proposed method uses the precorrected-FFT algorithm to reduce the storage and accelerate the matrix vector product of the far field. In order to make the precorrected-FFT algorithm can calculate the broadband characteristics of electrically large targets more quickly, the matrix interpolation method is used to interpolate the near-field matrix of the precorrected-FFT algorithm to improve the efficiency of calculation. The numerical results obtained validate the proposed method and its implementation in terms of accuracy and runtime performance.

Index Terms─ Broadband electromagnetic scattering, interpolation technique, near matrix, P-FFT.

I. INTRODUCTION

As an accurate numerical method, method of moments (MoM) is widely used to analyze various complex electromagnetic problems [1]. However, the storage and calculation of MoM are very large, which limits the scale of solution to the problem. In order to expand the solution scale of MoM, many fast algorithms based on MoM are developed. It can be divided into two categories: one is the algorithm related to the integral kernel, such as FMM [2], MLFMA [3-4] and MLGFIM [5], and a class of methods based on fast Fourier transform (FFT) (AIM, P-FFT, IE-FFT, etc. [6-14]). The other is matrix compression method, such as the adaptive cross approximation (ACA) algorithm [15-18], skeletonization [19], etc. The analysis of broadband electromagnetic scattering is very important for radar target stealth and identification engineering. However, it is necessary to obtain the broadband RCS data in radar target identification engineering. It will take a lot of time to solve the integral equation point by point at each frequency point in the whole frequency band by using MoM. In the process of obtaining the broadband electromagnetic characteristics of the target, the characterristics of these fast algorithms are different. The methods based on fast multipole mainly use the addition theorem of Green's function in free space, so it has the problem of "wavelet interruption". The methods based on fast Fourier transform (FFT) algorithm can be used in wide frequency band, but the calculation efficiency is not high if it is used directly. In the analysis of broadband electromagnetic problem, the grid of the highest frequency point is used to discretize the target surface, which saves the time of preprocessing. In addition, the electrical size of the target is constantly changing in the process of frequency sweeping calculation. Therefore, if the fast multipole method is adopted, the setting of the bottom box must be increased, which undoubtedly increases the storage capacity of the near-field matrix.

In this paper, the precorrected fast Fourier transform (FFT) algorithm combined with near-field matrix

Submitted On: April 30, 2021
Accepted On: July 6, 2021

https://doi.org/10.47037/2021.ACES.J.360716

interpolation technique is proposed to analyze the broadband electromagnetic characteristics of electrically large targets. The precorrected-FFT algorithm is used to speed up the solution of matrix vector multiplication. Moreover, the impedance matrix is stored sparsely, which reduces the memory requirement. At the same time, the matrix interpolation method is used to quickly fill the near matrix to improve the calculation speed.

II. METHOD OF MOMENTS OF ELECTROMANETIC FIELD

In order to solve the electric field integral equation (EFIE) and magnetic field integral equation (MFIE) numerically by the method of moments, firstly, the conductor surface is divided into triangles, and then the current density expressed by RWG basis function expansion is substituted:

$$\vec{E}^i(\vec{r})\big|_{\tan} = j\omega\mu\int_S [\vec{J}_S(\vec{r}\,') + \frac{1}{k^2}\nabla(\nabla'\cdot\vec{J}_S)] G(\vec{r},\vec{r}\,')d\vec{r}\,'\big|_{\tan}, \tag{1}$$

$$n\times\vec{H}^i = \frac{\vec{J}_S(\vec{r}\,')}{2} - n\times P.V.\int_S \vec{J}_S(\vec{r}\,') \times\nabla G(\vec{r},\vec{r}\,')d\vec{r}\,', \tag{2}$$

where P.V. in (2) is Cauchy Principal value integral.

By using the Galerkin method, the RWG basis function $\vec{f}_m(\vec{r})$ is used as the testing basis function to test the equations (1) and (2):

$$Z_{mn}^{EFIE} = jk\eta\int_{S_m} ds\vec{J}_m(\vec{r})\cdot\int_{S_n} G(\vec{r},\vec{r}')\vec{J}_n(\vec{r}')ds' - j\frac{\eta}{k}\int_{S_m} ds\left[\nabla\cdot\vec{J}_m(\vec{r})\right]\cdot\int_{S_n} G(\vec{r},\vec{r}')\left[\nabla\cdot\vec{J}_n(\vec{r}')\right]ds', \tag{3}$$

$$Z_{mn}^{MFIE} = \frac{1}{2}\int_{S_m}\vec{J}_m(\vec{r})\cdot\vec{J}_n(\vec{r})ds + \int_{S_m} ds\left[\hat{n}\times\vec{J}_m(\vec{r})\right]\cdot\int_{S_n}\nabla G(\vec{r},\vec{r}')\times\vec{J}_n(\vec{r}')ds', \tag{4}$$

where, k and $\eta=\sqrt{\mu/\varepsilon}$ denote the wave number and wave impedance in free space. $\vec{J}_m$ and $\vec{J}_n$ are the test function and the basis function, respectively, S_m and S_n are their support sets.

Equations (3) and (4) are a series of linear equations, which are abbreviated as follows:

$$\sum_{n=1}^{N} Z_{mn}I_n = V_m,\ m=1,2,\cdots,N, \tag{5}$$

The expression (5) in the form of vector can be more succinctly written as the following matrix equation:

$$ZI=V, \tag{6}$$

which includes unknown current density I, elements of impedance matrix Z and excitation vector V.

The single electric field integral equation and the single magnetic field integral equation may encounter the phenomenon of internal resonance when dealing with the closed structure. That is to say, MoM matrix formed by the electric field integral equation and the magnetic field integral equation is almost singular or has a large condition number at some frequency points. However, the resonance frequency of the electric field integral equation is different from that of the magnetic field integral equation. Therefore, the combination field integral equation (CFIE) is derived by linear combination of electric field integral equation and magnetic field integral equation:

$$CFIE = \gamma EFIE + (1-\gamma)\eta MFIE, \tag{7}$$

where, the parameter $\gamma(\in[0,1])$ is generally selected as 0.5. CFIE not only guarantees high precision, but also has small matrix condition number.

III. P-FFT ALGORITHM

In P-FFT, the basis function is projected onto the corresponding grid, and the potential of the basis function is obtained by interpolating the potential of the grid. Before applying the P-FFT, it is necessary to construct a cube containing the whole solution domain. The cube is evenly divided into a series of grids, and the grid is further evenly divided into a series of meshes.

Generally speaking, the P-FFT can be divided into four steps: projection, convolution, interpolation and precorrection. Finally, the P-FFT approximate expression of Z_{mn} is obtained:

$$Z_{mn}^{P-FFT} = (Z_{mn} - Z_{mn}^{(P-FFT)-far}) + Z_{mn}^{(P-FFT)-far} \cong Z_{mn}^{(P-FFT)-near} + Z_{mn}^{(P-FFT)-far}, \tag{8}$$

where the calculation formula of $Z_{mn}^{(P-FFT)-far}$ is:

$$Z_{mn}^{(P-FFT)-far} = R_m^T H W_n. \tag{9}$$

The projection operator W projects the basis function to the regular grid, the convolution operator H calculates the potential of the regular grid, and the interpolation operator R calculates the potential on the basis function according to the potential on the regular grid.

IV. INTERPOLATION TECHNIQUE OF MOM MATRIX

Over the entire frequency band, the MoM matrix element $Z_{mn}(f)$ is a function of frequency. Set the frequency variation range as $[f_l, f_h]$, the scatterer is discretized at the highest frequency, and adopt triangular

mesh. The wavelength at the highest frequency is recorded as λ_h. In this case, the expressions of matrix elements of EFIE and MFIE are as follows:

$$Z_{mn}^{E}(f_r)=\int_{S_m(\lambda_h)}ds\int_{S_n(\lambda_h)}ds'\Big[\vec{J}_m(\vec{r})\cdot\vec{J}_n(\vec{r}\,')k_r -\nabla_h\cdot\vec{J}_m(\vec{r})\nabla'_h\cdot\vec{J}_n(\vec{r}\,')\frac{1}{k_r}\Big]\frac{e^{-jk_rR}}{R}\frac{j\eta\lambda_h^2}{4\pi}, \quad (10)$$

$$Z_{mn}^{M}(f_r)=\Big[\int_{S_m(\lambda_h)}ds\vec{J}_m(\vec{r})\cdot\vec{J}_n(\vec{r})-\frac{1}{2\pi}\int_{S_m(\lambda_h)}ds \vec{J}_m(\vec{r})\cdot\hat{n}\times\int_{S_n(\lambda_h)}ds'\nabla_h\frac{e^{-jk_rR}}{R}\times\vec{J}_n(\vec{r}\,')\Big]\frac{\eta\lambda_h^2}{2}, \quad (11)$$

where, $k_r=2\pi f_r$, the normalized frequency is $f_r=f/f_h$ in the interval $[f_l/f_h,1]$. The following changes:

$$z_{mn}^{S}(f_r):=\frac{Z_{mn}^{S}(f_r)}{\lambda_h^2}, \quad (12)$$

where, the superscript *S* represents *E*, *M*, *C*.

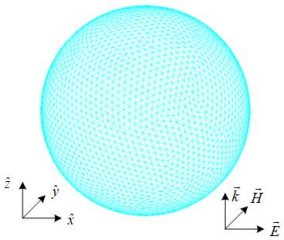

Fig. 1. A PEC sphere with radius $1.5\lambda_h$.

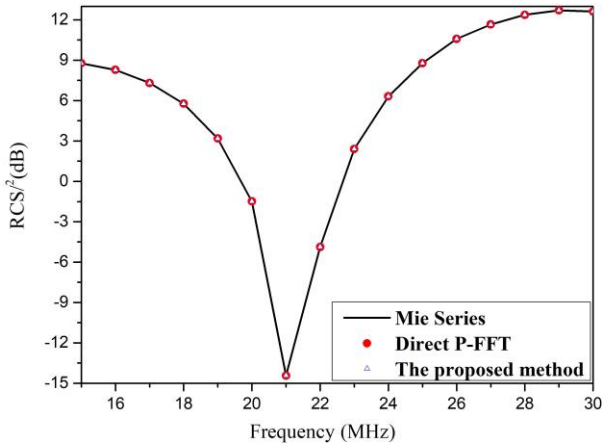

Fig. 2. Wide frequency band RCS curve of PEC sphere.

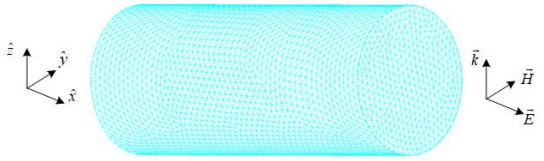

Fig. 3. A PEC cylinder with length $5\lambda_h$ and radius λ_h.

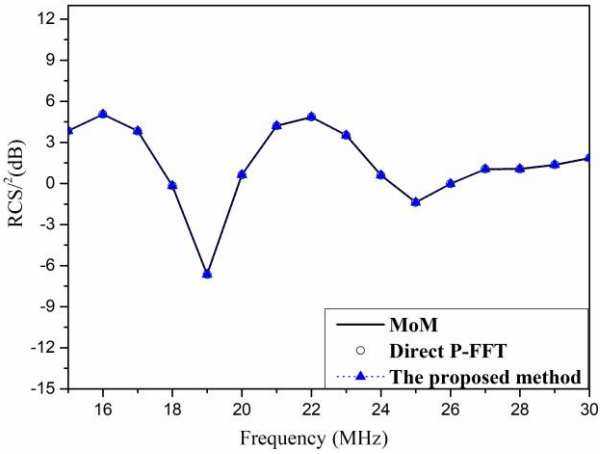

Fig. 4. Wide frequency band RCS curve of PEC cylinder.

Table 1: CPU time comparison of different algorithms for the three examples at 23 MHz (time: seconds)

Ex.	Method	Cartesian Grid Spacing	Filling Time of Z^{near}	Filling Time of the Near Part of Z^{far}
A	Direct P-FFT	$h=0.2\lambda_h$	21.6	0.5
	The proposed method	$h=0.2\lambda_h$	0.8	0.5
B	Direct P-FFT	$h=0.2\lambda_h$	19.6	0.4
	Triangle-Triangle	$h=0.2\lambda_h$	0.7	0.4
C	Direct P-FFT	$h=0.2\lambda_h$	15.2	0.3
	The proposed method	$h=0.2\lambda_h$	0.5	0.3
D	Direct P-FFT	$h=0.2\lambda_h$	166.2	3.8
	The proposed method	$h=0.2\lambda_h$	6.4	3.8
	AIM	$h=0.1\lambda_h$	146.1	3.1

Considering the fluctuation caused by the phase term e^{-jk_rR}, the correction matrix elements can be constructed as follows:

$$\tilde{z}_{mn}^{S}(f_r)=\begin{cases} z_{mn}^{S}(f_r)\, f_r e^{jk_r R_{mn}} & S_m \bigcap S_n = 0 \\ z_{mn}^{S}(f_r)\, f_r & S_m \bigcap S_n \neq 0 \end{cases}, \qquad (13)$$

where, the description of the relationship between S_m and S_n can be found in [20]. In this way, it becomes a quadratic polynomial about $\tilde{z}_{mn}^{S}(f_r)$.

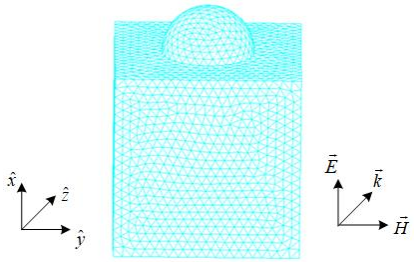

Fig. 5. A PEC combination of hemisphere and cube.

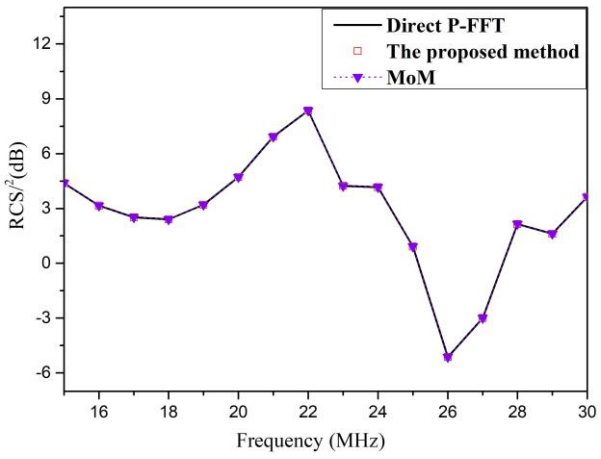

Fig. 6. Wide frequency band RCS curve of PEC combination of hemisphere and cube.

The modified matrices at $y_i = f_i / f_h$ $(i = 0,1,2,3;$ $f_i \in [f_l, f_h])$ which are optical frequency samples are generated primarily in the cubic polynomial inter/extrapolation method under investigation. The inter/extrapolation formula for each f_r is expressed as [21]:

$$\tilde{z}_{mn}^{S}(f_r)=\sum_{i=0}^{3}\tilde{z}_{mn}^{S}(y_i)\varphi_i(f_r), \qquad (14)$$

where

$$\varphi_i(f_r)=\prod_{j=0,\, j\neq i}^{j=3}\left(\frac{f_r-y_j}{y_i-y_j}\right), \qquad (15)$$

V. NUMERICAL RESULTS

In order to verify the correctness and efficiency of the proposed algorithm, some numerical examples are provided: a PEC sphere, a PEC cylinder, a PEC combination of hemisphere and cube and a PEC missile model. In all the examples, take the expansion order as $M = 2$. When the Cartesian grid spacing is at the highest frequency f_h, it is taken as $h_x = h_y = h_z = h$.

Example A: A PEC sphere

Consider a PEC sphere which's radius is $1.5\lambda_h$ with the incident angle of plane wave as shown in Fig. 1. The frequency range is [15 MHz, 30 MHz], and the frequency interval is $\Delta f = 1$ MHz. The surface of the sphere is discretized into triangular mesh with an edge length of about $\lambda_h / 10$. 10461 RWG basis functions are generated.

Figure 2 shows the broadband RCS curve with scattering angle $(\theta^s, \phi^s) = (40^o, 0^o)$ obtained by using the fast sweep frequency P-FFT algorithm. In the calculation, direct P-FFT with point-by-point calculation and the proposed method with interpolation technique are used. The results show that the two algorithms are in good agreement with the results of Mie series. Table 1 shows the time consumed by direct P-FFT and the proposed method at 23MHz. It can be seen that the latter significantly improves the computational efficiency. In this example, the proposed method takes 546.2 seconds to complete the full band calculation, while the direct with point-by-point calculation takes 810.1 seconds.

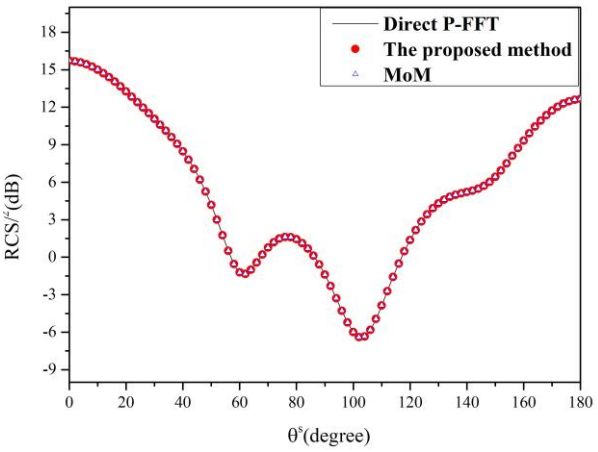

Fig. 7. Comparisons of the bistatic RCS of PEC combination of hemisphere and cube at 16MHz.

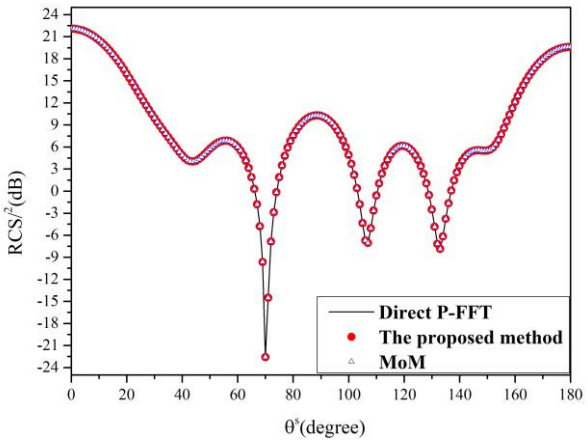

Fig. 8. Comparisons of the bistatic RCS of PEC combination of hemisphere and cube at 23MHz.

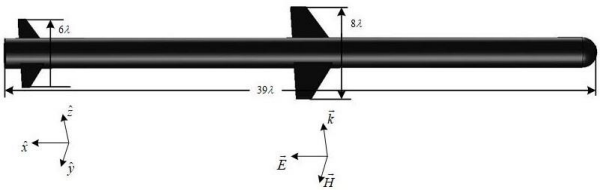

Fig. 9. A PEC missile model.

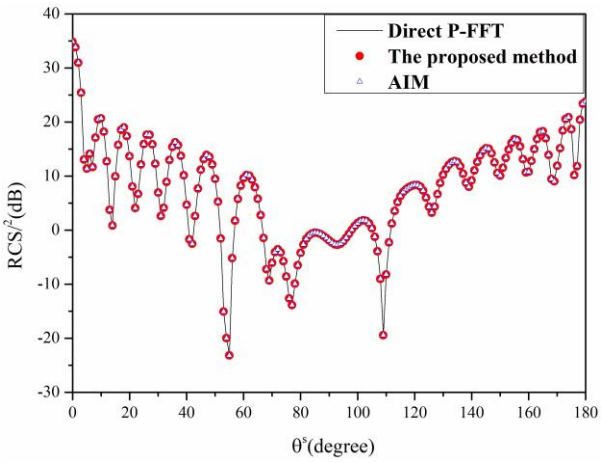

Fig. 10. Comparisons of the bistatic RCS of PEC missile model at 11MHz.

Example B: A PEC cylinder

A PEC cylinder of length $5\lambda_h$ and radius λ_h is shown in Fig. 3. The surface of the cylinder is discretized into triangular mesh with an edge length of $\lambda_h/10$ about 12675 RWG basis functions. The direction of incident plane wave and polarization direction of electric field are shown in Fig. 3. The frequency range is [15 MHz, 30 MHz], and the frequency interval is $\Delta f = 1$ MHz.

Figure 4 shows the broadband RCS curve with scattering angle $(\theta^s, \phi^s) = (70^o, 0^o)$ obtained by using the fast sweep frequency P-FFT algorithm. Direct P-FFT with point-by-point calculation, the proposed method with interpolation technique and MoM with point-by-point calculation are used in the calculation. By comparing the RCS obtained by the three algorithms, it shows that they are good agreement. Table 1 shows the time consumed by direct P-FFT and the proposed method with interpolation technique at 23 MHz. It can be seen that the latter significantly improves the computational efficiency. In this example, the proposed method with interpolation technique takes 695.2 secon-ds to complete the full band calculation, while the direct P-FFT takes 956.4 seconds.

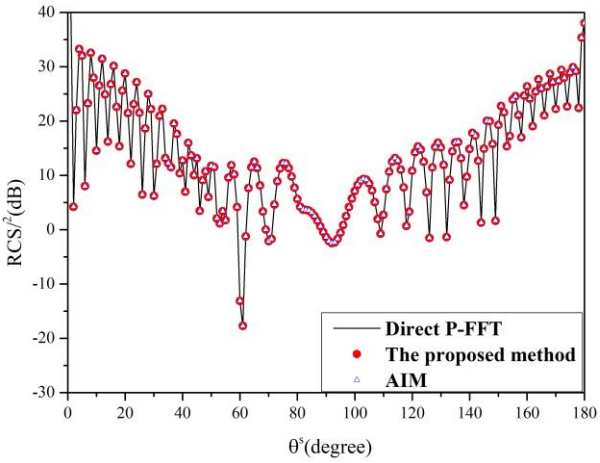

Fig. 11. Comparisons of the bistatic RCS of PEC missile model at 24MHz.

Example C: A PEC combination of hemisphere and cube

A combination model of a PEC hemisphere and a cube is considered. The surface of the combination model is discretized into triangular mesh, and its edge length is about $\lambda_h/10$. A total of 8471 RWG basis functions are generated, as shown in Fig. 5. The incident angle of incident plane wave is $(\theta^{in}, \phi^{in}) = (0^o, 0^o)$, and the polarization direction of electric field is shown in Fig. 5. The frequency range is [15 MHz, 30 MHz], and the frequency interval is $\Delta f = 1$ MHz.

Figure 6 shows the broadband RCS curve with scattering angle $(\theta^s, \phi^s) = (125^o, 0^o)$ obtained by using the fast sweep frequency P-FFT algorithm. Direct P-FFT with point-by-point calculation, the proposed method with interpolation technique and MoM with point-by-point calculation are used in the calculation. Figure 7 and Fig. 8 compare the bistatic RCS at 16 and 23MHz. It is observed that the results of the proposed

method agree very well with direct P-FFT and MoM. Table 1 shows the time consumed by direct P-FFT and the proposed method with interpolation technique at 23MHz. It can be seen that the latter significantly improves the computational efficiency. In this example, the proposed method with interpolation technique takes 710.1 seconds to complete the full band calculation, while the direct P-FFT takes 975.5 seconds.

Example D: A PEC missile

To examine the correctness of the proposed method, the broadband EM scattering from 5 to 30MHz of a PEC missile model shown in Fig. 9 is analyzed, and the frequency interval is $\Delta f = 1$ MHz. The model is discretized with 98475 RWG bases.

In Fig. 10 and Fig. 11, direct P-FFT with point-by-point calculation and AIM with point-by-point calculation are compared. Figure 10 and Fig. 11 illustrate the bistatic RCS curves at 11MHz and 24MHz, which differ from the interpolated nodes. The figure shows that the results of the proposed method are in good agreement with those of direct P-FFT point by point calculation and AIM. Related data of the three schemes are recorded in Table 1 at 23MHz. In this example, the proposed method with interpolation technique takes 4.1 hours to complete the full band calculation, while the direct P-FFT takes 5.2 hours. In this case, the proposed method with interpolation technique reduces the total CPU time by about 22% with almost no change in accuracy.

VI. CONCLUSION

In this paper, P-FFT and near-field matrix interpolation technique are combined to analyze the broadband scattering characteristics of targets. The matrix interpolation technique is introduced into P-FFT to improve the efficiency of near-field matrix filling, and avoid the problem that the traditional P-FFT takes too much time to calculate each frequency point. Finally, numerical results verify the correctness and effectiveness of the proposed method for calculating the broadband RCS of targets.

ACKNOWLEDGMENT

This work was supported partly by the National Natural Science Foundation of China under Grant 62071256, 11801492, The Natural Science Foundation of the Jiangsu Higher Education Institutions of China under Grant No. 18KJD510010, 19KJB120014, 19KJB510061, 19KJA110002, 20KJB140025.

REFERENCES

[1] R. F. Harrington, *Field Computation by Moment Methods*. New York, NY, USA: MacMillian, 1968.

[2] N. Engheta, W. D. Murphy, V. Rokhlin, and M. S. Vassiliou, "The fast multipole method (FMM) for electromagnetic scattering problems," *IEEE Trans. Antennas Propag.*, vol. 40, no. 6, pp. 634-641, June 1992.

[3] J.-M. Song, C.-C. Lu, and W. C. Chew, "Multi-level fast multipole algorithm for electromagnetic scattering by large complex objects," *IEEE Trans. Antennas Propag.*, vol. 45, no. 10, pp. 1488-1493, Oct. 1997.

[4] C. Delgado and F. Catedra, "Fast monostatic RCS computation using the near-field sparse approximate inverse and the multilevel fast multipole algorithm," *Applied Computational Electromagnetics Society*, vol. 35, no. 7, pp. 735-741, 2020.

[5] L. Li, H. G. Wang, and C. H. Chan, "An improved multilevel Green's function interpolation method with adaptive phase compensation," *IEEE Trans. Antennas Propag.*, vol. 56, no. 6, pp. 1381-1393, 2008.

[6] E. Bleszybski, M, Bleszynski, and T. Jaroszewicz, "AIM: Adaptive integral method for solving large-scale electromagnetic scattering and radiation problems," *Radio Science*, vol. 31, pp. 1225-1251, 1996.

[7] J. R. Phillips and J. K. White, "A precorrected-FFT method for electrostatic analysis of complicated 3-D structures," *IEEE Trans. Computer-Aided Design of Integrated Circuits and Systems*, vol. 16, pp. 1059-1072, 1997.

[8] W. J. Yu, C. H. Yan, and Z. Y. Wang, "Fast multi-frequency extraction of 3-D impedance based on boundary element method," *Microw. Opt. Tech. Lett.*, vol. 50, no. 8, pp. 2191-2197, 2008.

[9] C. F. Wang, F. Ling, and J. M. Jin, "A fast full-wave analysis of scattering and radiation from large finite arrays of microstrip antennas," *IEEE Trans. Antennas Propag.*, vol. 46, no. 10, pp. 1467-1474, Oct. 1998.

[10] S. Seung Mo and J. F. Lee, "A fast IE-FFT algorithm for solving PEC scattering problems," *IEEE Trans. Magn.*, vol. 41, no. 5, pp. 1476-1479, May 2005.

[11] M. Li, R. S. Chen, H. Wang, Z. Fan, and Q. Hu, "A multilevel FFT method for the 3-D capacitance extraction," *IEEE Trans. Comput. Aided Design Integr.*, vol. 32, no. 2, pp. 318-322, Feb. 2013.

[12] J. Y. Xie, H. X. Zhou, W. B. Kong, J. Hu, Z. Song, W. D. Li, and W. Hong, "A novel FG-FFT method for the EFIE," *Int. Conf. Comput. Problem-Solving (ICCP)*, 2012.

[13] J. Y. Xie, H. X. Zhou, W. Hong, W. D. Li, and G. Hua, "A highly accurate FGG-FG-FFT for the combined field integral equation," *IEEE Trans. Antennas Propag.*, vol. 61, no. 9, pp. 4641-4652, 2013.

[14] W. B. Kong, H. X. Zhou, K. L. Zheng, X. Mu, and W. Hong, "FFT-based method with near-matrix

compression," *IEEE Trans. Antennas Propag.*, vol. 65, no. 11, pp. 5975-5983, 2017.

[15] M. Li, T. Su, and R. S. Chen, "Equivalence principle algorithm with body of revolution equivalence surface for the modeling of large multiscale structures," *IEEE Trans. Antennas Propag.*, vol. 64, no. 5, pp. 1818-1828, 2016.

[16] M. Li, M. A. Francavilla, R. S. Chen, and G. Vecchi, "Wideband fast kernel-independent modeling of large multiscale structures via nested equivalent source approximation," *IEEE Trans. Antennas Propag.*, vol. 63, no. 5, pp. 2122-2134, 2015.

[17] H. X. Zhou, G. Y. Zhu, W. B. Kong, and W. Hong, "An upgraded ACA algorithm in complex field and its statistical analysis," *IEEE Trans. Antennas Propag.*, vol. 65, no. 5, pp. 2734-2739, 2017.

[18] A. Heldring, E. Ubeda, and J. M. Rius, "Stochastic estimation of the frobenius norm in the ACA convergence criterion," *IEEE Trans. Antennas Propag.*, vol. 63, no. 3, pp. 1155-1158, 2015.

[19] H. Rasool, J. Chen, X. M. Pan, and X. Q. Sheng, "Skeletonization accelerated solution of Crank-Nicolson method for solving three-dimensional parabolic equation," *Applied Computational Electromagnetics Society*, vol. 35, no. 9, pp. 1006-1011, 2020.

[20] W. D. Li, H. X. Zhou, W. Hong, and T. Weiland, "An accurate interpolation scheme with derivative term for generating MoM matrices in frequency sweeps," *IEEE Trans. Antennas Propag.*, vol. 57, no. 8, pp. 2376-2385, 2009.

[21] W. D. Li, H. X. Zhou, J. Hu, Z. Song, and W. Hong, "Accuracy improvement of cubic polynomial inter/extrapolation of MoM matrices by optimizing frequency samples," *IEEE Antennas Wireless Propag. Lett.*, vol. 10, pp. 888-891, 2011.